Acta Cryst. (1980). A**36**, 641–653

Anisotropy in Thermal Motion and in Secondary Extinction

BY R. J. NELMES

Department of Physics, University of Edinburgh, Mayfield Road, Edinburgh, EH9 3JZ, Scotland

(*Received* 7 *August* 1978; *accepted* 11 *February* 1980)

Abstract

Within certain good approximations the probability distribution function (p.d.f.) used to describe mosaic-block orientation in secondary-extinction models is exactly analogous to the p.d.f. for atomic thermal motion in the harmonic approximation. Use is made of this relationship to explain carefully, with the aid of several diagrams, certain distinctions and relationships common to both p.d.f.'s – which if not properly understood can lead (and have led) to some important confusions. For example, if the three-dimensional p.d.f. is Gaussian, surfaces of constant probability density are ellipsoidal (*e.g.* the thermal-vibration ellipsoid); but the scattering process 'sees' this p.d.f. as a *one*-dimensional projection, the half-width of which lies on a fourth-order surface (shaped, for example, like a peanut shell). For extinction it is shown explicitly that the form of this projected one-dimensional function is independent of experimental conditions (*e.g.* collimation), and that an earlier form [Coppens & Hamilton (1970), *Acta Cryst.* A**26**, 417–425], still commonly used and tested, is always incorrect. Apart from the intentional restriction of the detailed analysis of secondary extinction to type I extinction (in which mosaic-block orientation is the dominant effect), the approximations adopted are shown to have a wide range of validity. The (unusual) conditions under which the approximations may be sufficiently invalid to produce detectable effects are examined qualitatively in relation to the possibility of experimental investigations.

Introduction

In structure analysis the thermal motion of an atom is described by a three-dimensional probability distribution function (p.d.f.). In the harmonic approximation this p.d.f. is Gaussian and surfaces of constant probability density are then ellipsoidal – the familiar 'thermal-vibration ellipsoid'. Current models of secondary extinction also use a three-dimensional p.d.f. to describe mosaic-block orientation. Again, a Gaussian function is usually a good approximation, though a Lorentzian form is often found to give a significantly better fit to the data.

In both cases – thermal motion and extinction – the scattering process 'sees' a one-dimensional *projection* of the three-dimensional p.d.f. The thermal motion p.d.f. is 'seen' projected onto a line in the direction of the scattering vector, **S**; the mosaic-block orientation p.d.f. is 'seen' projected onto a line in the direction **D**, perpendicular to the scattering plane. If the three-dimensional p.d.f. is anisotropic, the one-dimensional distribution 'seen' will vary with the orientation of **S** (for thermal motion) or **D** (for secondary extinction) with respect to the three-dimensional function. That is to say, the one-dimensional projection (of the three-dimensional p.d.f.) itself varies in three dimensions. In the case of mosaic-block orientation this latter variation can be mapped out directly – for example by measuring rocking-curve widths.

There are thus two closely related but quite different three-dimensional functions to be understood and distinguished in considering anisotropic thermal motion and anisotropic secondary extinction. Importantly misleading confusion between the two can, and does, arise. One purpose of this article is to try, with the help of several diagrams, to make the distinction clear. In the case of secondary extinction, correctly relating *any* anisotropic model to experimental measurements (such as integrated intensities or rocking-curve widths) requires several other distinctions and relationships to be understood. These, too, are set out and discussed to try to clarify them.

Reference is made to two earlier papers in which such topics have been treated: first for thermal motion (Nelmes, 1969) and then for secondary extinction (Thornley & Nelmes, 1974). These treatments are here drawn together, illustrated and considerably extended – expanding on a preliminary form presented recently (Nelmes, 1977).

Distribution functions for thermal motion

The position of an atom executing thermal motion about its mean position is described by a probability

0567-7394/80/040641-13$01.00

distribution function (p.d.f.) in three dimensions. Let this p.d.f. be $p(x_1x_2x_3)$ such that the probability of the atom being in the volume element $\delta x_1\delta x_2\delta x_3$ (see Fig. 1 is $p(x_1x_2x_3)\delta x_1\delta x_2\delta x_3$, the product of the probability density at $(x_1x_2x_3)$ and a volume element around that point: x_1, x_2 and x_3 are coordinates relative to the principal axes X_1, X_2 and X_3. These local orthogonal axes, X_i, do not in general bear any necessary relation to the crystal axes. The p.d.f. must satisfy the normalization condition.

$$\int_{-\infty}^{\infty}\int\int p(x_1x_2x_3)\,dx_1\,dx_2\,dx_3 = 1;$$

and throughout this paper 'normalization' will be used in this sense of normalization to unity.

For harmonic thermal motion $p(x_1x_2x_3)$ is a Gaussian

$$p(x_1x_2x_3) = [(2\pi)^{3/2}u_1u_2u_3]^{-1} \times \exp[-\tfrac{1}{2}(x_1^2/u_1^2 + x_2^2/u_2^2 + x_3^2/u_3^2)], \quad (1)$$

where u_1, u_2 and u_3 are the root-mean-square displacements (r.m.s.d.) along the principal axes X_1, X_2 and X_3: that is, there is an equal probability of the atom being in a volume element displaced u_1 along X_1, u_2 along X_2 or u_3 along X_3 (Nelmes, 1969). The points $(\pm u_1\,0\,0)$, $(0\,\pm u_2\,0)$ and $(0\,0\,\pm u_3)$ thus lie on a surface of constant probability* in the function $p(x_1x_2x_3)$. In a general direction, **n**, the radius of this particular constant-probability surface is equal to the displacement along **n** which has the same probability as $\pm u_1$ along X_1 *etc.* A possible surface of constant probability is illustrated in Fig. 1. For a Gaussian p.d.f. the surface is an ellipsoid (Nelmes, 1969); and this is the so-called 'thermal-vibration ellipsoid' presented in descriptions of crystal structures.

The confusion that can arise is that these ellipsoids are sometimes *incorrectly* taken to represent the magnitude of the root-mean-square (or mean-square) displacement of atoms.

As a first step in examining how the mean-square displacement (m.s.d.) and root-mean-square displacement (r.m.s.d.) are correctly related to $p(x_1x_2x_3)$ it is helpful to distinguish the two (at least) ways of defining m.s.d. The temperature factor depends on the m.s.d. in the direction of the scattering vector **S**. If **n** is a unit vector along **S** (see Fig. 1), the m.s.d. can be

(*A*) the mean value of the square of the projection onto **n** of *all* displacements (m.s.d.*A*), or

(*B*) the mean value of the square of displacements within an elemental solid angle about **n** (m.s.d.*B*); such a solid angle is illustrated in Fig. 1 with a half-angle $\delta\alpha$. Thus, for example, displacements in the element $\delta x_1\delta x_2\delta x_3$ would be excluded from m.s.d.*B* for the scattering process illustrated.

Since diffraction is not sensitive to the position of a scatterer in the plane perpendicular to **S**, the appropriate definition in this context is clearly (*A*). That is to say, scattering 'sees' thermal motion as the one-dimensional distribution function for a displacement x along **n**, $p_A(x,\mathbf{n})$, obtained by projecting the whole distribution $p(x_1x_2x_3)$ perpendicularly onto **n**. As shown before (Nelmes, 1969),

$$p_A(x,\mathbf{n}) = [2\pi(u_1^2n_1^2 + u_2^2n_2^2 + u_3^2n_3^2)]^{-1/2} \times \exp[-\tfrac{1}{2}x^2/(u_1^2n_1^2 + u_2^2n_2^2 + u_3^2n_3^2)], \quad (2)$$

where n_i is the component of **n** along X_i. This is a normalized, one-dimensional Gaussian function. [Note the error, here corrected, in the normalization factor of the corresponding equation (9) in Nelmes (1969). Also there are some small changes in notation to reach a compromise between that of Nelmes (1969) and that of Thornley & Nelmes (1974): this is set out in the Appendix.]

Definition (*B*) can be shown (Nelmes, 1969) to yield the one-dimensional p.d.f.,

$$p_B(x,\mathbf{n}) = [(2\pi)^{3/2}u_1u_2u_3]^{-1} \times \exp[-\tfrac{1}{2}x^2(n_1^2/u_1^2 + n_2^2/u_2^2 + n_3^2/u_3^2)]\,\pi x^2(\delta\alpha)^2. \quad (3)$$

This is a bi-modal function [$p_B(x=0,\mathbf{n}) = 0$] and, of course, is *not* normalized (since only part of $p(x_1x_2x_3)$ is included). Although $p_B(x,\mathbf{n})$ is not relevant to the scattering process it is included because, as discussed later, it has proved helpful in understanding a recent confusion in the treatment of anisotropic secondary extinction.

Equations (2) and (3) are derived explicitly for a Gaussian $p(x_1x_2x_3)$. But the distinction between, and

* Probability *density*, strictly. But, for ease of expression, the distinction (made explicitly in the first paragraph of this section) is taken to be understood in formally equivalent contexts hereafter.

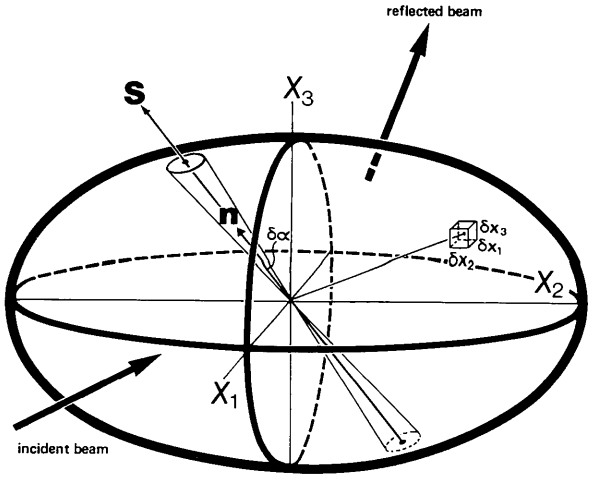

Fig. 1. A surface of constant probability (see previous footnote) in the probability distribution function for thermal motion. Symbols are defined in the text.

definition of, $p_A(x,\mathbf{n})$ and $p_B(x,\mathbf{n})$ apply to *any* form for the three-dimensional p.d.f.; and, *whatever* the form of $p(x_1x_2x_3)$, it is 'seen' in the diffraction process as $p_A(x,\mathbf{n})$.

Representational surfaces for thermal motion

For the case that the three-dimensional p.d.f., $p(x_1x_2x_3)$, is Gaussian the following results can be derived (Nelmes, 1969):

(i) constant probability lies on an ellipsoid (Fig. 1) – and, as said, this is the 'thermal-vibration ellipsoid';
(ii) m.s.d.A lies on a sixth-order surface;
(iii) r.m.s.d.A lies on a fourth-order surface; and
(iv) (r.m.s.d.A)$^{-1}$ lies on an ellipsoid – clearly different from (i) since it has dimensions L^{-1}: this ellipsoid is a surface of constant temperature factor (in reciprocal space).

Explicit forms for these representational surfaces are given in Nelmes (1969), together with corresponding results derived from definition (B).

Having pointed out the need to be quite clear about what is meant by m.s.d., attention is now focused on the relevant definition, (A); and the relationships between some principal representational surfaces are presented diagrammatically. Fig. 2(a) shows a surface (ellipsoid) of constant probability in an anisotropic p.d.f. for thermal motion with $u_3 > u_1 = u_2$; the semi-axial lengths are ku_i (*i.e.* proportional to u_i), and here, for simplicity of presentation, the particular case $k = 1$ is chosen. The corresponding (r.m.s.d. A)$^{-1}$ lies on an ellipsoid [see (iv) above] which, by definition, must have semi-axial lengths $1/u_i$: this is shown in Fig. 2(b). Then r.m.s.d.A lies on the fourth-order surface [(iii) above] that is the inverse of the (r.m.s.d.A)$^{-1}$ ellipsoid. This fourth-order representational surface for r.m.s.d.A has (by definition) semi-axial lengths u_i, and is shaped like a peanut shell as illustrated in Fig. 2(c).

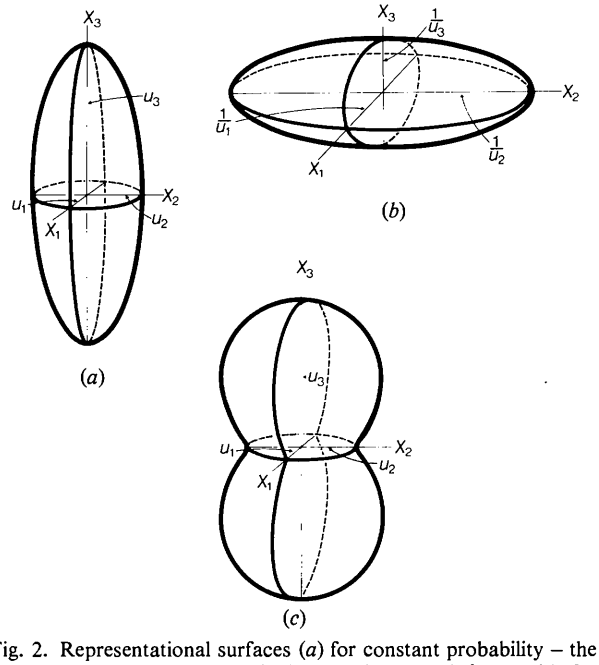

Fig. 2. Representational surfaces (a) for constant probability – the 'thermal-vibration ellipsoid', (b) for (r.m.s.d.A)$^{-1}$ and (c) for r.m.s.d.A, when $u_3 > u_1 = u_2$. *Note that here, and in Figs.* 3 *and* 5, *the horizontal* (X_1X_2) *sections are circular in every case. It is further noted that surfaces with the largest axial length vertical* (*Figs.* 2*a*, 2*c*, 3*b*, 5*a*, 5*c*) *have been drawn with a slightly different angle of view from that used for surfaces with the smallest axial length vertical* (*Figs.* 2*b*, 3*a*, 3*c*, 5*b*).

Consider the X_2 X_3 plane through the (r.m.s.d.A)$^{-1}$ ellipsoid. The trace of the surface in this plane is an ellipse of semi-axial lengths $1/u_2$ and $1/u_3$. It is a straightforward exercise to draw an ellipse, E, and convince oneself that a plot of the reciprocal of the radius of E is a shape like a figure eight – such as is shown in the X_2X_3 plane of Fig. 2(c). In the simple case chosen here, the surfaces are symmetric around the X_3 axis and so the full r.m.s.d.A surface has the peanut-shell form obtained by rotating the 'figure eight' around its long axis. The exercise with the ellipse will also show that the 'waisting' of the peanut shell becomes more pronounced as the (r.m.s.d.A)$^{-1}$ ellipsoid – and so the thermal-vibration ellipsoid – becomes more eccentric (anisotropic).

Fig. 3 illustrates in the same way the relationship between the representational surfaces for (a) constant probability, (b) (r.m.s.d.A)$^{-1}$ and (c) r.m.s.d.A when $u_3 < u_1 = u_2$. In contrast to Fig. 2, it can be seen that the 'figure eight' in the X_2X_3 plane of Fig. 3(c) now has its

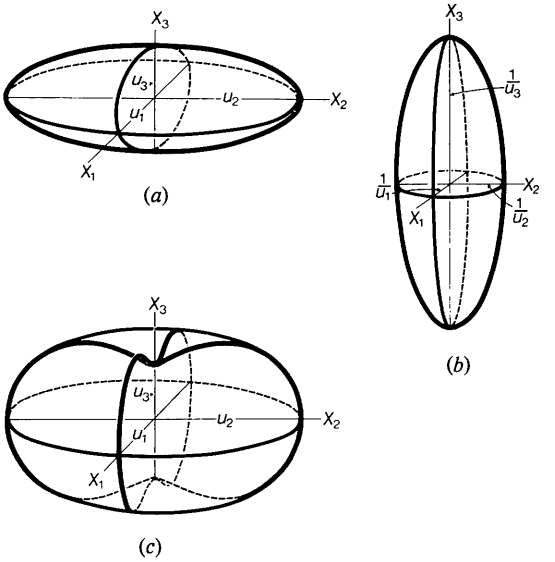

Fig. 3. Representational surfaces (a) for constant probability – the 'thermal-vibration ellipsoid', (b) for (r.m.s.d.A)$^{-1}$ and (c) for r.m.s.d.A, when $u_3 < u_1 = u_2$.

long axis along X_2. The surfaces are still symmetric around X_3, and so the representational surface for r.m.s.d.A in this case is obtained by rotating the 'figure eight' around its short axis. The resulting shape (Fig. 3*c*) could be described as a 'buttoned cushion'.*

In the general case, $u_1 \neq u_2 \neq u_3$, the fourth-order surface will be more complex. But it will retain the characteristic that each of its three principal sections will have the 'figure eight' shape – the sharpness of the waisting increasing with the eccentricity of the ellipse in the corresponding section of the (r.m.s.d.A)$^{-1}$ ellipsoid.

The important distinction – which it is the first aim of the paper to convey – is that between, on the one hand, a representational surface of constant probability of thermal displacement (Figs. 2*a* and 3*a*) and, on the other hand, the surface that represents the variation in three dimensions of the root-mean-square-(A) of such displacements (Figs. 2*c* and 3*c*). The surfaces (*a*) represent the variation in three dimensions of a *three*-dimensional distribution, $p(x_1x_2x_3)$, whereas surfaces (*c*) represent the variation in three dimensions of (the width of) the *one*-dimensional distribution, $p_A(x,\mathbf{n})$, obtained as a projection of $p(x_1x_2x_3)$.

It is clear that whilst the semi-axial lengths of surfaces (*a*) and (*c*) are in the same proportion (here shown equal), their shapes can be very different indeed. But, because the radius of the thermal-vibration ellipsoid *is* proportional to r.m.s.d.A in the principal directions (Figs. 2*a* and 3*a*), it is easy to make the error of taking this surface to represent r.m.s.d.A in a general direction – rather than the correct form shown in Figs. 2(*c*) and 3(*c*). [Another path to the incorrect expectation that r.m.s.d. will lie on an ellipsoid may start from an implicit choice of definition (B) for m.s.d.]

Finally, attention is drawn to the fact that, whilst the thermal-vibration ellipsoid has semi-axial lengths *proportional* to u_1, u_2 and u_3, it is otherwise related to the parameters of thermal motion in an unspecified way unless the particular surface of constant probability given is defined. In Figs. 2(*a*) and 3(*a*) a surface with semi-axial lengths *equal* to u_1, u_2 and u_3 has been chosen just, as said, to simplify the comparison with Figs. 2(*c*) and 3(*c*). But when the results of structure analyses are presented graphically, with drawings of the thermal-vibration ellipsoids, these ellipsoids are usually scaled to include 50% probability [*i.e.* the included volume is such that $\int_V p(x_1x_2x_3)\mathrm{d}x_1\mathrm{d}x_2\mathrm{d}x_3 = 0{\cdot}5$]; the semi-axial lengths of the ellipsoid are then $1{\cdot}54\ u_i$ (Willis & Pryor, 1975, p. 98). There is thus no single, uniquely defined thermal-vibration ellipsoid: it is simply one of the possible surfaces of constant probability in $p(x_1x_2x_3)$.

* The descriptions 'peanut shell' for the shape of Fig. 2(*c*) and 'buttoned cushion' for that of Fig. 3(*c*) are not technical! – and may not convey familiar images to all readers. The purpose is simply to provide an easy way of referring to these two very different forms of the representational surface for r.m.s.d.A (and, later, r.m.s.m.A).

Distribution functions for mosaic-block orientation

The interpretation of anisotropic thermal motion has been rehearsed first, not only to extend and illustrate earlier work (Nelmes, 1969) but because, being more straightforward, it affords a useful introduction to the description of anisotropic secondary extinction.

In this description the crystal is taken to be composed of mosaic blocks that are (on average) ellipsoidal in shape. In the most recent formulation, due to Becker & Coppens (1974, 1975), the size of this average mosaic block enters the calculation as the parameter $\bar{\alpha}$, proportional to $r(\mathbf{u})$ the radius of the ellipsoid in the direction $\mathbf{u}$ of the scattered beam. Equation (8) of Becker & Coppens (1975) gives $\bar{\alpha} = \frac{3}{2}r(\mathbf{u})\sin 2\theta/\lambda$: the representational surface for $\bar{\alpha}$ is thus the same ellipsoid as describes the average mosaic-block shape, except that it is scaled by $\frac{3}{2}\sin 2\theta/\lambda$ (see also Thornley, 1980). It does not seem likely, then, that important confusion will arise between $\bar{\alpha}$ and $r(\mathbf{u})$. But, as discussed in detail by Thornley (1980), the broadening function, $B(\mathbf{D})$ – on which type II extinction directly depends – is obtained from the mosaic-block shape (reduced to $\bar{\alpha}$) *via* Fourier transformation (Becker & Coppens, 1974, 1975). This broadening function [$B(\mathbf{D})$ in the notation of this paper (see the Appendix): $\mathbf{D}$ is defined below] then has a half-width that varies as $1/r(\mathbf{u})$ (see Thornley, 1980); since $r(\mathbf{u})$ lies on an ellipsoid, it can be seen from the arguments of the previous section that the half-width of $B(\mathbf{D})$ will map out in three dimensions a shape such as Fig. 2(*c*) or 3(*c*). However, in the main part of this paper it is assumed – as will usually be true (see Becker, 1977) – that the half-width of $B(\mathbf{D})$ is rather small compared with that of the other relevant distribution, the distribution of mosaic-block orientations. This is equivalent to making the approximation that the secondary extinction is entirely type I. Departures from this approximation are certainly important and are discussed, in terms of the effect of the $B(\mathbf{D})$ function, in a later section. But for a detailed discussion of the exact form of $B(\mathbf{D})$, the representational surface for its half-width, and how this may be manifested in experimental measurements the reader is referred to Thornley (1980).

Attention is focused here, then, on the problems that can and do arise in the use and interpretation of an anisotropic distribution of mosaic-block *orientations*.

The orientation of mosaic blocks can be described by a p.d.f. in three dimensions, $p(\Delta_1\Delta_2\Delta_3)$, where Δ_i is a rotation about the principal axis X_i and $\Delta_1 = \Delta_2 = \Delta_3 = 0$ corresponds to the mean orientation taken over all blocks. (The axes X_i bear no necessary relationship to the crystal axes.) To simplify the presentation here, $p(\Delta_1\Delta_2\Delta_3)$ is taken to be Gaussian – but essentially the same arguments could be followed through for any form (*e.g.* a Lorentzian). The Gaussian form [compare

with (1)] is

$$p(\Delta_1\Delta_2\Delta_3) = [(2\pi)^{3/2}\sigma_1\sigma_2\sigma_3]^{-1} \times \exp[-\tfrac{1}{2}(\Delta_1^2/\sigma_1^2 + \Delta_2^2/\sigma_2^2 + \Delta_3^2/\sigma_3^2)], \quad (4)$$

where σ_1, σ_2 and σ_3 are the root-mean-square misorientations (r.m.s.m.) around the principal axes: that is, there is an equal probability of a mosaic block being misoriented (relative to the mean) σ_1 about X_1, σ_2 about X_2 or σ_3 about X_3. As before, the surface of constant probability is an ellipsoid, as illustrated in Fig. 4 – for the same spatial relationship of incident beam, scattering vector **S**, and reflected beam as in Fig. 1.

The meaning of this distribution function is perhaps harder to grasp than that of the p.d.f. for thermal displacement. For what follows it is important to recognize clearly that displacement from the origin of the function along, for example, the X_3 direction corresponds to increasing rotation Δ_3 *around* X_3: the value of the function at some point Δ_3 along the X_3 axis, $p(0\,0\,\Delta_3)$, is thus the fraction of mosaic blocks, per unit volume of the crystal, that is misoriented through an angle Δ_3 only and exactly about X_3. Then the value of the function at a general point $(\Delta_1\Delta_2\Delta_3)$ is the fraction of mosaic blocks misoriented exactly Δ_1 about X_1, Δ_2 about X_2 and Δ_3 about X_3. [It should be noted here that all misorientation angles for mosaic blocks will be taken to be small enough to add as vectors.] To keep the interpretation of $p(\Delta_1\Delta_2\Delta_3)$ as simple as possible, it will be assumed, without further comment, that it is physically plausible to interpret the misorientation, Δ, of a mosaic block (from the mean orientation) simply as a real rotation through Δ. This essentially attributes mosaic-block misorientation solely to local bending of the reflecting planes and neglects the effect of local variations of d spacing. The latter would give rise to θ- and wavelength-dependent effects.

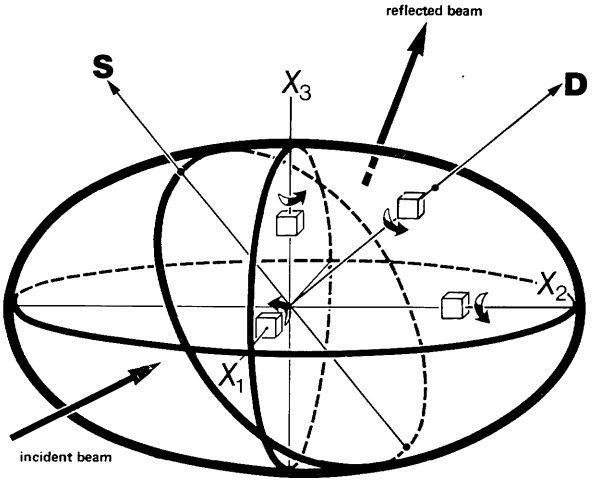

Fig. 4. A surface of constant probability in the probability distribution function for mosaic-block orientation. The plane shown passing through the origin and containing **S** is the median co-reflecting surface for the scattering process illustrated. The small cubes show a possible convention for the sense of rotation (from the mean orientation) with increasing displacement from the origin. Other symbols are defined in the text.

As with thermal motion, it is now necessary to consider how this p.d.f. is 'seen' in a scattering process. An integrated intensity is measured by rotating the crystal, and so the distribution $p(\Delta_1\Delta_2\Delta_3)$, about some axis **R**. In conventional four-circle diffractometer geometry **R** is coincident with **D**, the normal to the scattering plane (the plane containing the incident beam, the scattering vector **S** and the reflected beam). In non-zero-layer measurements using normal-beam geometry **R** is inclined to **D** by an amount that varies from reflection to reflection. This introduces some complications (discussed later), but no differences in principle from the results obtained with **R** and **D** coincident. To avoid inessential complexity at this stage, then, detailed discussion will be restricted to the case **R** = **D**.

Then it is important to make a clear distinction between (i) how much the reflected beam is *extinguished* and (ii) how much of the reflected intensity is *measured* (*i.e.* enters the detector). Extinction essentially depends on the interaction between the crystal and each incident photon (or neutron). For secondary extinction (within the limit of the Darwin transfer equations) what matters is, first, how many mosaic blocks are so oriented as to be in the reflecting position [relative to some incident photon (neutron) direction, $\mathbf{k}_0$], and secondly the probability that any one of these mosaic blocks will reflect. The first factor depends on (i) the size, shape and orientation of the crystal, (ii) the number of mosaic blocks per unit volume of the crystal, (iii) the form of $p(\Delta_1\Delta_2\Delta_3)$ and its orientation relative to $\mathbf{k}_0$ and (iv) – as discussed later but neglected at this stage – broadening effects [such as $B(\mathbf{D})$ above]. The second factor depends on (i) Q [proportional to $\lambda^3F^2(hkl)Lp$, where λ is the incident wavelength, $F(hkl)$ is the structure amplitude and Lp is the Lorentz–polarization factor], (ii) the average mosaic-block volume and, again, (iii) broadening effects – which, as suggested earlier and discussed in detail by Thornley (1980), depend mainly on the average size, shape and orientation of the mosaic blocks. The essential point to take from this is that the amount of extinction does *not* depend on the collimation of either the incident or the reflected beam. In a real experiment the incident beam is divergent and the reflected beam, even for a perfectly collimated incident beam, is divergent. If the whole integrated intensity is to be measured, all of the reflected beam for each of the directions in the (divergent) incident beam must enter the detector. Such considerations are important, of course, and are discussed later. But here the question

addressed – and the question on which secondary extinction entirely depends if broadening effects are neglected – is how the p.d.f., $p(\Delta_1\Delta_2\Delta_3)$, is 'seen' by incident photons (neutrons) in a given scattering process (from a given crystal in a given orientation).

So, for the present purposes, these simplifying assumptions can helpfully be introduced: (i) that the incident beam is perfectly collimated, (ii) that the intrinsic reflection width of mosaic blocks [*i.e.* the half-width of $B(\mathbf{D})$] is negligible and (iii) that the crystal is spherical. With these assumptions, all the factors listed in the preceding paragraph as affecting secondary extinction are reduced to only one that varies in a scan (about **D**) through a given reflection – namely the orientation of $p(\Delta_1\Delta_2\Delta_3)$ relative to $\mathbf{k}_0$. Starting from the peak of the reflection the scattering process illustrated in Fig. 4 will then 'see' $p(\Delta_1\Delta_2\Delta_3)$ in the following sequence:

(i) all points in the plane shown in Fig. 4, perpendicular to **D** and passing through the origin, represent mosaic blocks with zero misorientation about **D**, and so (to a very good approximation) they scatter together – at the peak of the reflection;

(ii) then all points in an adjacent parallel plane represent mosaic blocks which have the same (small) misorientation, Δ, about **D**, and so scatter together – a little off the peak of the reflection, when the crystal has been rotated Δ about **D**;

(iii) and so on.

Thus, with the assumptions made, one plane (of mosaic-block orientations) at a time is picked out of $p(\Delta_1\Delta_2\Delta_3)$; and these planes are perpendicular to **D**.

It is in fact only an approximation – though, as said under (i) immediately above, a very good one – to treat these 'planes' as strictly planar. More exactly, these 'planes' have a small curvature (the same for all of them) around a line parallel to **S**, superimposed on which there is a second, even smaller curvature (zero for the plane shown in Fig. 4, and increasing away from it) around a line parallel to $\mathbf{N} = \mathbf{D} \times \mathbf{S}$. However, the departure from strict planarity is negligible except at high scattering angles with crystals which have a very wide mosaic spread (say 30′). The further (very good) approximation is thus made that the surfaces successively picked out of $p(\Delta_1\Delta_2\Delta_3)$, as it is rotated about **D**, are exactly planar. These surfaces will be referred to hereafter as 'co-reflecting surfaces' or, if the context is unambiguous, as 'planes'.

Thus, to a very good approximation, in a scan about **D** $p(\Delta_1\Delta_2\Delta_3)$ is sampled in successive 'planes' perpendicular to **D**. It is then clear that the one-dimensional distribution function 'seen' in the scattering process is $p(\Delta_1\Delta_2\Delta_3)$ projected perpendicularly onto **D**. This one-dimensional function, $p_A(\Delta,\mathbf{D})$, is thus related to $p(\Delta_1\Delta_2\Delta_3)$ *exactly* as $p_A(x,\mathbf{n})$ is related to $p(x_1x_2x_3)$; and so [compare with (2)]

$$p_A(\Delta,\mathbf{D}) = [2\pi(\sigma_1^2 d_1^2 + \sigma_2^2 d_2^2 + \sigma_3^2 d_3^2)]^{-1/2} \times \exp[-\tfrac{1}{2}\Delta^2/(\sigma_1^2 d_1^2 + \sigma_2^2 d_2^2 + \sigma_3^2 d_3^2)], \quad (5)$$

where d_i is the component of **D** along X_i. This is a normalized, one-dimensional Gaussian function. Though this explicit form for $p_A(\Delta,\mathbf{D})$ is derived for a Gaussian form for $p(\Delta_1\Delta_2\Delta_3)$ [see (4)], the prescription stated above for the derivation of $p_A(\Delta,\mathbf{D})$ is entirely general – it applies *whatever* the form of $p(\Delta_1\Delta_2\Delta_3)$.

Representational surfaces for mosaic-block orientation

If $p(\Delta_1\Delta_2\Delta_3)$ is Gaussian it is clear that the results quoted already for thermal motion will apply, namely:

(i) constant probability lies on an ellipsoid (*e.g.* Fig. 4);

(ii) mean-square misorientation (A) (m.s.m.A) lies on a sixth-order surface;

(iii) r.m.s.m.A lies on a fourth-order surface; and

(iv) (r.m.s.m.A)$^{-1}$ lies on an ellipsoid.

Since the forms of, and relationships between, these surfaces are exactly as already discussed for thermal motion, only one illustration is given. Fig. 5 shows the analogue of Fig. 2, with σ_i replacing u_i and $\sigma_3 > \sigma_1 = \sigma_2$ – the case that gives a peanut-shell-shaped surface for r.m.s.m.A (Fig. 5*c*). [The case $\sigma_3 < \sigma_1 = \sigma_2$ will yield a 'buttoned-cushion' shape for the r.m.s.m.A surface, as illustrated for r.m.s.d.A in Fig. 3*c*.]

Again, the important distinction to be made is that between Fig. 5(*a*) – a surface of constant probability in

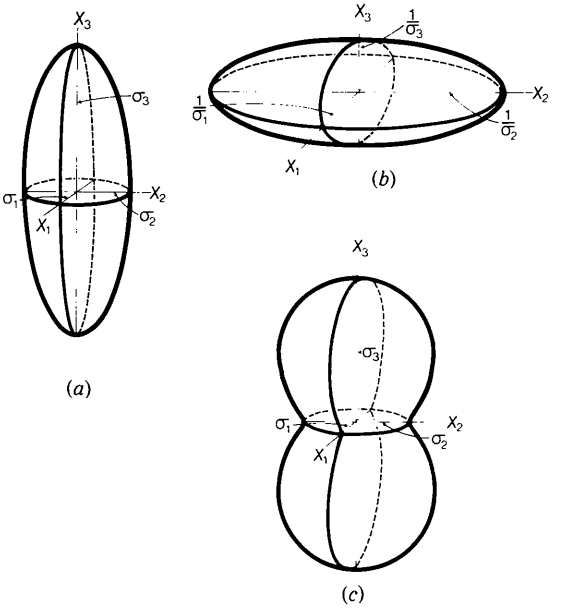

Fig. 5. Representational surfaces (*a*) for constant probability of mosaic-block orientation, (*b*) for (r.m.s.m.A)$^{-1}$ and (*c*) for r.m.s.m.A, when $\sigma_3 > \sigma_1 = \sigma_2$.

the three-dimensional function $p(\Delta_1\Delta_2\Delta_3)$, and Fig. 5(*c*) – the surface that represents the variation in three dimensions of r.m.s.m.A, the width of the one-dimensional function $p_A(\Delta,\mathbf{D})$. Failure to make this distinction can be a bountiful source of confusion, especially as the r.m.s.m.A surface can be mapped out by making measurements of rocking-curve widths. A rocking curve about **D**, when deconvoluted from the resolution function, is a direct measure of $p_A(\Delta,\mathbf{D})$. [This, like other statements in this section, is strictly true only within the (generally good) approximations adopted in deriving $p_A(\Delta,\mathbf{D})$ in the preceding section.]

Indeed, some rocking-curve measurements made recently by Lehmann & Schneider (1977) beautifully illustrate the principal points made so far in this paper. The measurements were performed on plastically deformed single crystals of copper, and the rocking-curve widths for successive orientations round the scattering vector were found to vary as illustrated schematically in Fig. 6 (the scattering vector is perpendicular to the plane of the diagram; the rocking-curve width is greatest for a scan about X_3 and least for a scan about X_1). In three dimensions these measurements mapped out a strongly-waisted, peanut-shell-shaped surface, quite symmetric about its long axis.

This result was at first interpreted as showing the three-dimensional mosaic-block orientation p.d.f. to be highly non-Gaussian (Lehmann & Schneider, 1977) – essentially because the authors initially tried to use the (incorrect) Coppens–Hamilton (1970) form for the one-dimensional distribution 'seen' in the scattering process, a form that predicts an ellipsoidal surface for r.m.s.m. (as explained in the following section). In fact, their observations afford a striking illustration of the distinction that has to be made between the constant-probability surface and the r.m.s.m.A surface. The surface they found is very much like that shown in Fig. 5(*c*) except that it is more strongly waisted and not quite symmetric about the long axis. This, then, is entirely consistent with a Gaussian-like* $p(\Delta_1\Delta_2\Delta_3)$ that is quite strongly anisotropic ($\sigma_3 \gg \sigma_1 \simeq \sigma_2$).

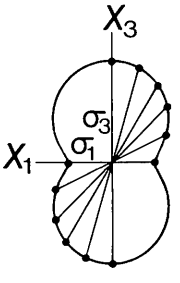

Fig. 6. A schematic representation of the typical variation of rocking-curve width (●——● is the width for a scan about the direction of ●——●), with rotation round the scattering vector, found by Lehmann & Schneider (1977) in a plastically deformed single crystal of copper.

In a note at the end of their paper, Lehmann & Schneider (1977) accept this in relation to the similar, though less strongly waisted, peanut-shell surface they derive from their crystal-structure refinements. They remark, though, that the difference between the predictions of the Coppens–Hamilton form and of $p_A(\Delta,\mathbf{D})$ – which they denote $P_2(\Delta,\mathbf{D})$ – has generally been assumed to be small for weak extinction. This raises a further important point. No doubt it is true that such an assumption is often made, but it is incorrect because it fails to distinguish the mosaic-block distribution from the strength of extinction. The latter depends not only on the magnitudes of σ_i but also on experimental conditions such as the wavelength and type (X-ray or neutron) of the radiation used, the size of the crystal and so on; the former is a constant, intrinsic property of the crystal and depends *only* on the relative magnitudes of σ_1, σ_2 and σ_3. It is thus possible, probably common, to have very weak extinction and yet a highly anisotropic mosaic-block distribution – as Lehmann & Schneider (1977) so convincingly show.

The Coppens–Hamilton formulation

Corresponding to the distribution $p_B(x,\mathbf{n})$ for thermal motion, it is possible to define a distribution, $p_B(\Delta,\mathbf{D})$, which includes mosaic-block misorientations about axes lying only within a solid angle (of half-angle $\delta\alpha$) around **D**. For the case that $p(\Delta_1\Delta_2\Delta_3)$ is Gaussian,

$$p_B(\Delta,\mathbf{D}) = [(2\pi)^{3/2}\sigma_1\sigma_2\sigma_3]^{-1} \exp\,[-\tfrac{1}{2}\Delta^2(d_1^2/\sigma_1^2 + d_2^2/\sigma_2^2 + d_3^2/\sigma_3^2)]\,\pi\Delta^2(\delta\alpha)^2, \quad (6)$$

which, of course, is the same as (3) with x replaced by Δ, u_i by σ_i and n_i by d_i. Equation (6) [or (3)] describes a bi-modal distribution – as must any form for the $p_B(\Delta,\mathbf{D})$ [or $p_B(x,\mathbf{n})$] distribution – and is not normalized since it includes only a small part of $p(\Delta_1\Delta_2\Delta_3)$.

Although the p_B one-dimensional distributions do not correspond to any possible diffraction experiment they are helpful here. It is shown in Nelmes (1969) that r.m.s.d.B (and so, also, r.m.s.m.B) lies on an ellipsoidal surface for a Gaussian $p(x_1x_2x_3)$ [or $p(\Delta_1\Delta_2\Delta_3)$]. It is thus possible to identify two paths to the incorrect expectation that r.m.s.m. should lie on an ellipsoid for a Gaussian three-dimensional p.d.f.: first by confusing

* These rocking-curve measurements must 'see' an overall p.d.f. that includes the macroscopic bending of the copper crystals (Lehmann & Schneider, 1977). The expected effects would be to introduce some 'flattening' as well as extension of the intrinsic p.d.f. along the bending axis. However, if there is a 'flattening' component in this case it does not appear to be significant enough to obscure the illustration these measurements afford of the point being made here.

the (fourth-order) surface of r.m.s.m. with the (ellipsoidal) surface of constant probability, and secondly by choosing, implicitly or explicitly, a definition of m.s.m. that predicts an ellipsoidal surface for r.m.s.m.

An important example of the second path being taken is in the formulation of anisotropic extinction advanced by Coppens & Hamilton (1970). Their treatment assumes mosaic-block orientation to be described by a Gaussian function in three dimensions, but then uses for the one-dimensional distribution the form

$$p_{B'}(\Delta,\mathbf{D}) = [(2\pi)^{-1}(d_1^2/\sigma_1^2 + d_2^2/\sigma_2^2 + d_3^2/\sigma_3^2)]^{1/2} \times \exp[-\tfrac{1}{2}\Delta^2(d_1^2/\sigma_1^2 + d_2^2/\sigma_2^2 + d_3^2/\sigma_3^3)]. \quad (7)$$

This normalized, Gaussian distribution function incorporates two mistakes:

(i) as first pointed out by Thornley & Nelmes (1974), it excludes from reflection mosaic blocks with *any* component of misorientation about an axis other than **D**;* and

(ii) a distribution that thus picks out from the three-dimensional p.d.f. only an elemental cylinder around **D** loses any clear meaning (in relation to the three-dimensional p.d.f.) if it is normalized: its 'proper form' is

$$p_{B''}(\Delta,\mathbf{D}) = [(2\pi)^{3/2}\sigma_1\sigma_2\sigma_3]^{-1}\exp[-\tfrac{1}{2}\Delta^2(d_1^2/\sigma_1^2 + d_2^2/\sigma_2^2 + d_3^2/\sigma_3^2)]\,\pi(\mathrm{d}r)^2, \quad (8)$$

where dr is the cylinder radius. However, because $p_{B'}(\Delta,\mathbf{D})$ *is* normalized, it can be seen [(5) and (7)] that $p_{B'}(\Delta,\mathbf{D})$ and $p_A(\Delta,\mathbf{D})$ are identical for the special cases of **D** along X_1, X_2 or X_3. In these special cases the predictions of the Coppens–Hamilton form, $p_{B'}(\Delta,\mathbf{D})$, and the Thornley–Nelmes form, $p_A(\Delta,\mathbf{D})$, agree (accidentally) because of cancelling errors in the former.

A comparison of (6) and (7) shows that $p_B(\Delta,\mathbf{D})$ and $p_{B'}(\Delta,\mathbf{D})$ differ only in their normalization factors and the isotropic term Δ^2; and so r.m.s.m.B', like r.m.s.m.B, lies on an ellipsoidal surface. Altogether, then, the Coppens–Hamilton formulation uses a distribution $p_{B'}(\Delta,\mathbf{D})$ which does not in particular, and cannot in general, correspond to any experiment, and which for a Gaussian $p(\Delta_1\Delta_2\Delta_3)$ predicts an ellipsoidal representational surface for r.m.s.m. Hence (probably) the initial expectation of Lehmann & Schneider (1977) that their rocking-curve measurements of r.m.s.m. should lie on an ellipsoid and their initial (incorrect) conclusion that the actual peanut-shell shape revealed a highly non-Gaussian $p(\Delta_1\Delta_2\Delta_3)$.

* The exponential term in (7) is simply (proportional to) the product of the probabilities for those three component misorientations which correspond to a resultant misorientation of Δ about **D**.

It is not the wish or intention to labour one small error in the important advance made by Coppens & Hamilton (1970). The object is solely to demonstrate convincingly that it *is* an error. Since this was shown by Thornley & Nelmes (1974), quite a number of experimental papers have compared the fit obtained with the Coppens–Hamilton and Thornley–Nelmes 'formulations' as if they were competing models. But the latter authors are of the opinion that this is barren labour: it seems plain enough that Coppens & Hamilton (1970) were simply in error over this one point, and this has been accepted in the more recent published work of Coppens (Becker & Coppens, 1975). If the point needs more experimental demonstration than already given by Thornley & Nelmes (1974), the results of Lehmann & Schneider (1977) seem more than adequately convincing.

Thornley (1980) has shown that in advancing the case for $p_A(\Delta,\mathbf{D})$ as against $p_{B'}(\Delta,\mathbf{D})$ an error was made by Thornley & Nelmes (1974). It has been reproduced, reasonably enough, in the note at the end of Lehmann & Schneider (1977); and also in Nelmes (1977) and in the recent comprehensive reformulation of extinction theory by Becker & Coppens (1974, 1975). Although none of the positive conclusions reached is affected, this error may have contributed to the continued use of the Coppens–Hamilton formulation by suggesting conditions (albeit impossible to achieve) under which that formulation could be valid. The mistake turned on a failure to make the distinction discussed already between how much the reflected beam is extinguished and how much of the reflected beam enters the detector. Thus collimation was thought, incorrectly, to be relevant to the appropriate choice of the one-dimensional function, and it was wrongly stated that $p_{B'}(\Delta,\mathbf{D}) - p_1(\Delta,\mathbf{D})$ in the notation of Thornley & Nelmes (1974) – corresponds to perfect collimation of the incident beam. But, as now shown more carefully here (see also Thornley, 1980), the appropriate one-dimensional function is *always* $p_A(\Delta,\mathbf{D})$. Collimation has no effect whatever on how $p(\Delta_1\Delta_2\Delta_3)$ is 'seen' in the scattering process; it affects only how much of the reflected beam is detected – a quite separate topic which is discussed in the following section.

A second, closely related, error appears in Nelmes (1977): it is incorrectly surmized that $p_B(\Delta,\mathbf{D})$ could be 'seen' in a highly collimated experiment.

Collimation conditions for integrated-intensity and rocking-curve measurements

Consider a perfectly collimated experiment: that is to say, the incident beam is confined to the one direction $\mathbf{k}_0$ and the reflected beam to the one direction $\mathbf{k}$ (by an extremely small aperture at the detector). **S**, $\mathbf{k}_0$ and $\mathbf{k}$ lie in the scattering plane, all exactly perpendicular to **D**.

Fig. 7 shows again a surface of constant probability in $p(\Delta_1\Delta_2\Delta_3)$, with the same scattering geometry as Fig. 4. At the peak of the reflection, mosaic blocks with zero misorientation about **D** and *all* possible misorientations about **S** (*i.e.* line *AA'*) will reflect *into the detector*. The last three words are crucial: at this position of the crystal (the peak of the reflection) mosaic blocks with all orientations in the co-reflecting surface through $p(\Delta_1\Delta_2\Delta_3)$ shown in Fig. 4 will *reflect*, but not, with the collimation assumed, into the detector. [Points away from the line **S** in the co-reflecting surface (Fig. 4) represent misorientations with some rotation about the direction $\mathbf{N} = \mathbf{D} \times \mathbf{S}$. These will give rise to reflected beams which are to one side or the other of the scattering plane – and so are excluded from this detector.] If the crystal is now turned through a small angle Δ about **D**, mosaic blocks with exactly this angle, Δ, of misorientation about **D** and all possible misorientations about the direction parallel to **S** (*i.e.* line *BB'*) will reflect into the detector.

It can be seen, then, that with very tight collimation the mosaic-block orientations that can reflect into the detector in a full scan lie in the plane containing **S** and **D**, as shown in Fig. 7. [This surface is not exactly a plane; but, except for extreme cases, it is very closely planar, and can certainly be assumed to be so for the present argument.] Such a measurement clearly does not record the integrated intensity: the full extent of $p(\Delta_1\Delta_2\Delta_3)$ along **D** is scanned, but not along **N**.

If the collimation is relaxed, mosaic blocks with small misorientations about **N** can reflect into the detector – which thus 'sees' a slice through $p(\Delta_1\Delta_2\Delta_3)$ centred on the plane, shown in Fig. 7, containing **S** and **D**. For the measurement of complete integrated intensity this slice must be wide enough to include the whole significant extent of $p(\Delta_1\Delta_2\Delta_3)$ in the **N** direction. And for some possible forms of $p(\Delta_1\Delta_2\Delta_3)$, such as a Lorentzian, this requirement may well not be fulfilled by what are considered 'normal' apertures if the specimen crystal has a moderately large mosaic spread.

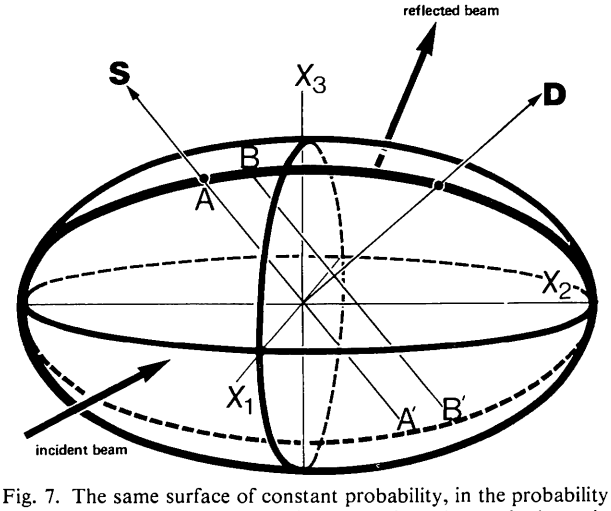

Fig. 7. The same surface of constant probability, in the probability distribution function for mosaic-block orientation, as is shown in Fig. 4. The orientations that can reflect into the detector in a perfectly collimated (and aligned) experiment lie in the plane shown passing through the origin, and containing **S** and **D**. Other symbols are defined in the text.

This point about possible partial masking of the full integrated intensity by an insufficiently large receiving aperture is not advanced as anything new (see Denne, 1977, for example). It is included here to help clarify a distinction made earlier that is crucial to the main part of this paper – namely that between how much of $p(\Delta_1\Delta_2\Delta_3)$ is 'seen' by an incident beam (which is what matters for extinction) and how much of $p(\Delta_1\Delta_2\Delta_3)$ is 'seen' by the detector (which is what matters for measurement of integrated intensity, and also rocking curves). The fact that under conditions of tight collimation only part of the reflected beam enters the detector makes no difference to the amount by which the reflected beam is extinguished.

Thus it is that extinction is determined *always*, under *all* conditions, by $p_A(\Delta,\mathbf{D})$.

The collimation conditions for the detector to measure the whole integrated intensity amount to the conditions for the detector to 'see' all of $p_A(\Delta,\mathbf{D})$. So, not only in measuring integrated intensities but also – perhaps more so – in experiments such as those of Lehmann & Schneider (1977) it is important that these conditions be met. If they are not, then the rocking curves (deconvoluted from the resolution function) are no longer direct measures of $p_A(\Delta,\mathbf{D})$; and the widths obtained cannot be related directly to the parameters of $p(\Delta_1\Delta_2\Delta_3)$.

The validity of the approximations; and experimental investigations

In the case of thermal motion the only approximation made is that the motion is harmonic and so $p(x_1x_2x_3)$ is Gaussian. Very often the p.d.f. is significantly anharmonic (indeed, in principle, it can never be exactly harmonic) and so non-Gaussian. The *explicit* results discussed earlier are thus in some measure approximate – to exactly the degree that the 'thermal-vibration ellipsoid' is approximate. But what is of primary concern here is the relationship between $p(x_1x_2x_3)$, whatever its form, and how it is 'seen' in a scattering process: and the statement that it is always 'seen' as $p_A(x,\mathbf{n})$, obtained by projecting $p(x_1x_2x_3)$ perpendicularly onto **n**, stands as an entirely general prescription.

The discussion of secondary extinction contains many more approximations. These are summarized – (1) to (5) – in this paragraph and then, in turn, discussed in detail. (1) Overall looms the assumption that the microstructure of real crystals can be approxi-

mated reasonably (or, at least, parameterized adequately) by a distribution of orientations of an average perfect mosaic block – where the distribution function is analytic (Gaussian or Lorentzian) and uniform throughout the crystal, and the average mosaic block has an ellipsoidal shape. (2) In discussing how $p(\Delta_1\Delta_2\Delta_3)$ is 'seen' in the scattering process the incident beam has been taken to be perfectly collimated; and (3) the effects of the intrinsic dynamic width of Bragg reflections and of their diffraction broadening have been neglected. Under these conditions, an incident photon (or neutron) 'sees' as aligned to reflect all those mosaic blocks whose orientations lie in an infinitesimally thin surface through $p(\Delta_1\Delta_2\Delta_3)$; this 'co-reflecting surface' is perpendicular to **D** where it crosses **D** and, as described earlier, is slightly curved; but (4) these surfaces have been taken to be exactly planar. (5) Finally, only the simple case of four-circle geometry has been discussed, in which the rotation axis is always **D**.

(1) In one sense the mosaic-block model is obviously a very poor one: a real crystal cannot be entirely composed of ellipsoidal mosaic blocks packed together. But here again a clear distinction must be borne in mind, which is perhaps an important one for all work in this area. The essential purpose of extinction models has *not* been to provide an accurate description of real crystal microstructure, but to model adequately that difference between observed and calculated integrated intensities which is attributed to extinction. The achievement of the latter does not necessarily depend on a knowledge or incorporation of the former: in a helpful review of the range of applicability of extinction models, Becker (1977) shows that the mosaic-block model gives results surprisingly close to those achieved recently (with far greater labour) from more fundamental theories. There are thus good empirical grounds for accepting the mosaic-block approximation for the present (and many other) purposes.

The assumption that $p(\Delta_1\Delta_2\Delta_3)$ is analytic and uniform is often strikingly wrong as shown, for example, in γ-ray rocking-curve measurements (see, in particular, Schneider, 1977). Highly non-uniform mosaic structure seems to arise from mutual misalignment of regions of the crystal that are large in comparison with mosaic blocks. Such characteristics are thus much more likely to be encountered in crystals of the dimensions used in neutron-diffraction experiments than in X-ray diffraction. When the mosaic structure *is* uniform it seems to be described well by a Gaussian or Lorentzian form (Lehmann & Schneider, 1977; Becker & Coppens, 1975); when it is significantly non-uniform the standard, analytic model becomes an approximation, possibly a bad one. Again, *how* bad rather depends on whether the objective is a good statistical description of crystal microstructure or an adequate extinction correction. The long-range inhomogeneities revealed in the γ-ray rocking curves are probably less important than they might appear to be for extinction in integrated intensity measurements – when smaller crystals are often used and the relevant interaction with the crystal occurs over a distance within which the mosaic structure is more nearly uniform (Becker, 1977). This exposes a difficulty with the concept of a $p(\Delta_1\Delta_2\Delta_3)$ function as a definite, intrinsic property of a given crystal: different experimental measurements (γ-ray rocking curves, neutron-diffraction rocking curves, extinction refinements) may 'see' different p.d.f.'s (Lehmann & Schneider, 1977). So, once the mosaic structure departs from being ideally uniform, $p(\Delta_1\Delta_2\Delta_3)$ has to be defined in relation to a particular type of measurement; and clearly this must be borne in mind in comparing different measurements. However, given a $p(\Delta_1\Delta_2\Delta_3)$ defined by a particular experiment, no matter how non-uniform the mosaic structure, the general prescription for relating this $p(\Delta_1\Delta_2\Delta_3)$ to $p_A(\Delta,\mathbf{D})$ remains valid. Thus the restriction* in this paper to consideration of a uniform mosaic structure described by a Gaussian form of p.d.f. is not, in itself, an approximation: it is just a particular, possible example.

(2) The incident beam has been taken to be perfectly collimated (and monochromatic). This is equivalent to deconvoluting the resolution function. Since, as has been stressed, extinction essentially depends on the interaction between each incident photon (neutron) and $p(\Delta_1\Delta_2\Delta_3)$ as 'seen' by it, this assumption is not – in this context – an approximation. But, of course, the divergence (in space and wavelength) of the primary beam must be taken into account in deconvoluting $p_A(\Delta,\mathbf{D})$ from rocking-curve measurements, and in considerations of collimation conditions for the measurement of whole integrated intensities [and $p_A(\Delta,\mathbf{D})$].

(3) Even for a large, perfect crystal a Bragg reflection has a finite intrinsic width – of the order of a few seconds of arc (James, 1967). And in a mosaic crystal, reflections from each mosaic block will be diffraction-broadened in inverse proportion to the size of the mosaic block along **u**, the scattered-beam direction (see above and Thornley, 1980). For many crystals the 'width' of $p(\Delta_1\Delta_2\Delta_3)$ is less than a minute of arc; at most, it is a few minutes of arc. So any incident photon (neutron) can, in fact, diffract from all mosaic blocks whose orientations lie in adjacent co-reflecting surfaces of $p(\Delta_1\Delta_2\Delta_3)$ over a finite range along **D**: this range depends on the intrinsic width and the diffraction broadening in relation to the width of $p(\Delta_1\Delta_2\Delta_3)$ along **D**. The intrinsic width has, approximately, the form of a rectangle function (James, 1967); the diffraction-broadening function $B(\mathbf{D})$ introduced

* The fact that the crystals used by Lehmann & Schneider (1977) do not conform to this restriction, being macroscopically bent, does not invalidate the use made of their results, because there was no comparison between measurements of different types.

earlier has long Lorentzian-like tails (Thornley, 1980). The combined effect (by convolution) will be a broadening function, $B'(\mathbf{D})$, which is wider than $B(\mathbf{D})$ by the intrinsic width, but otherwise (usually) of a closely similar form. With $B'(\mathbf{D})$ taken into account, the one-dimensional function 'seen' in the scattering process becomes $p_{A'}(\Delta,\mathbf{D})$, the convolution of $p_A(\Delta,\mathbf{D})$ with $B'(\mathbf{D})$. When $B'(\mathbf{D})$ is somewhat narrower than $p_A(\Delta,\mathbf{D})$ the latter function will dominate the convolution. Then $p_{A'}(\Delta,\mathbf{D})$ will have a form very similar to that of $p_A(\Delta,\mathbf{D})$ and they will differ little in width. Under these conditions the approximation used in the earlier part of this paper [that $p_{A'}(\Delta,\mathbf{D})$ and $p_A(\Delta,\mathbf{D})$ are the same – *i.e.* that type I extinction predominates] is a good one. And it has been shown that these conditions are indeed those more commonly encountered in practice, especially when extinction is severe (Becker, 1977). In the remaining cases, where the widths of $B'(\mathbf{D})$ and $p_A(\Delta,\mathbf{D})$ are comparable, the Lorentzian-like tails of $B'(\mathbf{D})$ will mean that $p_{A'}(\Delta,\mathbf{D})$ is not only significantly wider than $p_A(\Delta,\mathbf{D})$ but also is of a significantly different form.*

It is worth considering how $B(\mathbf{D})$ and $p_A(\Delta,\mathbf{D})$ functions of comparable width are handled in refinements of the Becker & Coppens (1974, 1975) models. Often there is too much parameter correlation to refine together the parameters of $p(\Delta_1\Delta_2\Delta_3)$ and those describing the average mosaic-block (shape) ellipsoid. Then two separate refinements are carried out: type I in which the parameters of $p(\Delta_1\Delta_2\Delta_3)$ are refined, taking the diffraction-broadening width to be zero; and type II in which the parameters of the average mosaic-block ellipsoid are refined, taking the width of $p(\Delta_1\Delta_2\Delta_3)$ to be zero. The refinement that gives the better fit is accepted as the best that can be done. But note that the achievement of a satisfactory fit does not necessarily mean that the widths taken to be zero are even *small*. For the other situation, in which the parameters of $p(\Delta_1\Delta_2\Delta_3)$ and the average mosaic-block ellipsoid *can* be refined together, it has been found necessary (and adequate) to introduce the approximation that the complex form of $B(\mathbf{D})$ is taken to be Lorentzian if a Lorentzian form of $p(\Delta_1\Delta_2\Delta_3)$ is being refined, and Gaussian if a Gaussian form of $p(\Delta_1\Delta_2\Delta_3)$ is being refined (Becker & Coppens, 1974). This is entirely acceptable insofar as it achieves (as it usually does) the central purpose of providing a good model of *how much* extinction happens – rather than how or why it happens. But the possibility of reaching clear conclusions about the underlying distributions may be forfeited. For example, $B(\mathbf{D})$ could be wide enough and of a sufficiently Lorentzian-like form that the Lorentzian/Lorentzian model yields a better fit though $p(\Delta_1\Delta_2\Delta_3)$ is actually Gaussian. Similar remarks apply, *a fortiori*, to the first-mentioned case where only the separate type I or type II refinements can be achieved, unless it can be demonstrated independently that the distribution assumed to have zero width is indeed very narrow.

From this discussion, it is evident that when the width of $B'(\mathbf{D})$ is at all comparable with that of $p_A(\Delta,\mathbf{D})$ it becomes very difficult to separate the two functions – both in rocking-curve measurements and in the refinement of current extinction-model parameters. The approximation made in this paper [that $B'(\mathbf{D})$ has negligible width] is thus a reasonable one, not only in terms of simplification of presentation and what happen to be the more commonly encountered experimental conditions (see above), but also in terms of the conditions under which direct investigations of $p(\Delta_1\Delta_2\Delta_3)$ are likely to be interpretable. [The other tractable case, $B'(\mathbf{D})$ very much wider than $p_A(\Delta,\mathbf{D})$, would be of considerable interest – though rather rare.]

(4) It has been explained earlier that, though the co-reflecting surfaces in $p(\Delta_1\Delta_2\Delta_3)$ are not exactly planar, their curvature is small and unlikely to yield any detectable effect except for rather large mosaic spreads (30′ or so) at high scattering angles. Any error in the estimate of extinction can be neglected because these conditions are precisely ones under which extinction is itself negligible. It can be shown that the effect of this (usually negligible) curvature of the co-reflecting surfaces will be to skew $p_{A'}(\Delta,\mathbf{D})$ to an asymmetric form, $p_{A''}(\Delta,\mathbf{D})$. Strictly, then, there is a quite complex relationship between $p_{A''}(\Delta,\mathbf{D})$ – the exact one-dimensional distribution function accessible to experimental measurement, and $p_A(\Delta,\mathbf{D})$ – its approximate form, obtained as a simple projection of $p(\Delta_1\Delta_2\Delta_3)$. Given the type I condition that $p_{A'}(\Delta,\mathbf{D})$ and $p_A(\Delta,\mathbf{D})$ are sensibly identical, the difference between $p_{A''}(\Delta,\mathbf{D})$ and $p_A(\Delta,\mathbf{D})$ is, as said, almost certainly unimportant for the purposes of modelling extinction; but the distinction need not be negligible for measurements (*e.g.* rocking curves) that are to be interpreted in terms of the precise form of $p(\Delta_1\Delta_2\Delta_3)$.

(5) Finally, consideration should be given to the effect of scanning about an axis $\mathbf{R}$ that is not coincident with $\mathbf{D}$. The most important point to make is that the one-dimensional distribution 'seen' by the scattering process remains $p_A(\Delta,\mathbf{D})$ – with this again now used as an approximation for $p_{A''}(\Delta,\mathbf{D})$. This is evident from the consideration that at any point in the scan about $\mathbf{R}$ the process does not 'know' whether $p(\Delta_1\Delta_2\Delta_3)$ is being turned about $\mathbf{R}$ or $\mathbf{D}$. The only difference is that when $\mathbf{R} \neq \mathbf{D}$ the direction of $\mathbf{D}$ is changing during the scan. Thus the co-reflecting surfaces successively picked out

* In such circumstances a crystal with an entirely Gaussian $p(\Delta_1\Delta_2\Delta_3)$ could yield non-Gaussian rocking curves, because of the effect of the broadening function. And the shape mapped out in three dimensions by the widths of such rocking curves could be rather complex, being compounded of two representational surfaces – (i) for r.m.s.m.A, and (ii) for the variation in three dimensions of the half-width of $B(\mathbf{D})$ – which need have no simple relationship with respect to size, detailed shape or relative orientation.

of $p(\Delta_1\Delta_2\Delta_3)$ are perpendicular to a line which follows a curved path through $p(\Delta_1\Delta_2\Delta_3)$. This means that a reflection scanned about $\mathbf{R} \neq \mathbf{D}$ will be broader than the same reflection scanned about **D**. The extinction will be altered in a way that depends on the detailed relative geometries of the **R** and **D** scans for each particular case. But, except for extreme geometries where the scan about **R** is exceptionally wide, the orientation of **D** will change little during the scan and the width and extinction will be little altered.

The reciprocal-space description

The discussion of $p(\Delta_1\Delta_2\Delta_3)$ in this paper has been in terms of an abstract space – in that displacement along a line, say **D**, in $p(\Delta_1\Delta_2\Delta_3)$ represents a *rotation* round **D**. In preparing the paper it has proved helpful to make frequent use of reciprocal-space constructions, though the two-dimensional nature of the reciprocal-space representation limits its usefulness in discussing and illustrating the essentially three-dimensional properties of $p(\Delta_1\Delta_2\Delta_3)$ and the related functions.

Also, the relationship between the two representations is not altogether straightforward. In reciprocal space the p.d.f. of mosaic-block orientations becomes a two-dimensional function centred on the mean direction of **S** and lying on a spherical surface of radius $|\mathbf{S}|$ – a 'spherical cap'. The co-reflecting surface in $p(\Delta_1\Delta_2\Delta_3)$ now becomes a co-reflecting line which is the locus of intersection of the 'spherical cap' with the Ewald sphere. Perhaps the most important point to remember in relating the two representations is that misorientations about a direction, say **D**, appear *along* **D** in $p(\Delta_1\Delta_2\Delta_3)$ but appear along a direction perpendicular to **D** in reciprocal space.

Summary

Attention has been drawn to two points at which care is needed in considering anisotropy: first in deriving from the three-dimensional distribution function the one-dimensional function appropriate to the experimental conditions, and secondly in understanding how the corresponding directly-measurable quantities (*e.g.* r.m.s.m.) relate to the parameters of the three-dimensional function (*e.g.* σ_1, σ_2 and σ_3). These considerations have been examined in detail for harmonic thermal motion and for mosaic-block orientation in secondary-extinction models. In both cases it is necessary to make the following distinctions carefully:

(i) the definition of mean-square thermal displacement (or mosaic-block misorientation) relevant to the scattering process as against other conceivable definitions; and

(ii) the variation in three dimensions of the three-dimensional p.d.f. (*e.g.* the ellipsoid of constant probability) as against the variation in three dimensions of the one-dimensional distribution 'seen' by the scattering process (*e.g.* the peanut-shell-shaped surface).

In the case of extinction it has been argued that these further distinctions need to be made:

(iii) how much the scattered beam is extinguished (independent of collimation) as against how much of the scattered beam is measured (*i.e.* passes through the detector aperture);

(iv) the strength of the extinction (dependent on experimental conditions) as against the anisotropy of the mosaic-block orientation (an intrinsic property of the crystal); and

(v) the essential purpose of extinction models of achieving an adequate modelling of the extinction *per se* (*i.e.* without necessary regard to true crystal microstructure, or even, perhaps, to obtaining the same parameters from the same crystal in different experiments) as against the purpose of experiments specifically intended to investigate and model true crystal microstructure.

From (i) and (iii) above it has been shown that $p(\Delta_1\Delta_2\Delta_3)$ is always 'seen' in the scattering process as $p_A(\Delta,\mathbf{D})$ and that the form, $p_{B'}(\Delta,\mathbf{D})$, suggested by Coppens & Hamilton (1970) is always incorrect.

The detailed discussion of distribution functions for secondary extinction has been circumscribed by a number of approximations – closely equivalent to the conditions under which the Becker & Coppens (1974, 1975) formalism works well and type I extinction dominates. The only significant restriction is thus the comparatively little attention given to diffraction broadening (type II extinction). For a discussion of the distribution functions involved in this latter case the reader is referred to Thornley (1980). The other restrictions and approximations have been shown to be reasonable for all but unusual, extreme cases; but they have been examined in relation to their possible relevance to detailed experimental investigations. It is concluded that it is prudent to restrict investigations of mosaic-block orientation to crystals with (*a*) the width of $B'(\mathbf{D})$ very much less than that of $p_A(\Delta,\mathbf{D})$ and (*b*) a very uniform mosaic structure.

Throughout the preparation of this paper I have enjoyed the generous advice and encouragement of Dr F. R. Thornley. I gratefully acknowledge detailed constructive criticism of the first draft by Dr M. S. Lehmann and Dr J. Hutton; also suggestions for small amendments to the final version from Dr G. J. McIntyre, Professor W. Cochran, Professor D. W. J. Cruickshank and Professor A. Vos; and some kind assistance with mathematical problems from Dr A. D.

Bruce. The diagrams were executed by Mr J. McNeill of Edinburgh University's Audio-Visual Services: I am glad to record my thanks to him for his patient and painstaking work.

APPENDIX

To avoid unnecessary confusion, some differences of notation between this paper and those to which it refers are set out. Earlier papers are abbreviated to N for Nelmes (1969), TN for Thornley & Nelmes (1974) and BC for Becker & Coppens (1974, 1975).

(i) This paper	N	TN	BC
$p_A(x,\mathbf{n})$	$p_A(X_1)$		
$p_B(x,\mathbf{n})$	$p_B(X_1)$		
$p_A(\Delta,\mathbf{D})$		$P_2(\Delta,\mathbf{D})$	$W'(\varepsilon_1,\mathbf{D})$
$p_{B'}(\Delta,\mathbf{D})$		$P_1(\Delta,\mathbf{D})$	$W(\varepsilon_1,\mathbf{D})$
$B(\mathbf{D})$			$\sigma(\varepsilon_1)$

(ii) In the discussion of diffraction broadening [the $B(\mathbf{D})$ function] the reflected beam direction is denoted $\mathbf{u}$ in accord with BC; elsewhere it is denoted $\mathbf{k}$.

References

BECKER, P. (1977). *Acta Cryst.* A**33**, 243–249.

BECKER, P. & COPPENS, P. (1974). *Acta Cryst.* A**30**, 129–147, 148–153.

BECKER, P. & COPPENS, P. (1975). *Acta Cryst.* A**31**, 417–425.

COPPENS, P. & HAMILTON, W. C. (1970). *Acta Cryst.* A**26**, 71–83.

DENNE, W. A. (1977). *Acta Cryst.* A**33**, 438–440.

JAMES, R. W. (1967). *The Optical Principles of the Diffraction of X-rays*, 7th reprinting, p. 58. London: Bell.

LEHMANN, M. S. & SCHNEIDER, J. S. (1977). *Acta Cryst.* A**33**, 789–800.

NELMES, R. J. (1969). *Acta Cryst.* A**25**, 523–526.

NELMES, R. J. (1977). Fourth Europ. Crystallogr. Meet., Abstract PI. 35, p. 162.

SCHNEIDER, J. R. (1977). *Acta Cryst.* A**33**, 235–243.

THORNLEY, F. R. (1980). *Acta Cryst.* Submitted.

THORNLEY, F. R. & NELMES, R. J. (1974). *Acta Cryst.* A**30**, 748–757.

WILLIS, B. T. M. & PRYOR, A. W. (1975). *Thermal Vibrations in Crystallography*. Cambridge: University Press.

Acta Cryst. (1980). A**36**, 653–656

The Application of Direct Methods to Centrosymmetric Structures containing Heavy Atoms. III

BY PAUL T. BEURSKENS, PETER A. J. PRICK AND TH. E. M. VAN DEN HARK

Crystallography Laboratory, Toernooiveld, 6525 ED Nijmegen, The Netherlands

AND R. O. GOULD

Edinburgh University, Department of Chemistry, West Mains Road, Edinburgh EH9 3JJ, Scotland

(*Received* 21 *November* 1979; *accepted* 11 *February* 1980)

Abstract

Direct methods are applied to difference-structure factors for a structure containing one or more heavy atoms at known special or pseudo-special positions, such that the heavy atoms do not contribute to several reflection parity groups. Phases of reflections in these parity groups, represented by symbols, are analysed by the sign-correlation method. Phases as well as amplitudes of the difference-structure factors are refined by the general *DIRDIF* procedure as described previously.

Introduction

In paper II (Gould, Van den Hark & Beurskens, 1975), direct methods were used to improve the phases as well as the amplitudes of the difference-structure factors. Experience with this procedure and application of similar procedures to non-centrosymmetric structures (Van den Hark, Prick & Beurskens, 1976; Prick, Beurskens & Gould, 1978) showed how to improve the procedure for the special case given in paper I (Beurskens & Noordik, 1971). In this special case the known atoms do not contribute to several reflection

0567-7394/80/040653-04$01.00